Iron Release Is Reduced by Mutations of Lysines 206 and 296 in Recombinant N-Terminal Half-Transferrin†

Lauren M. Steinlein,‡ Cathleen M. Ligman, Stacy Kessler, and Richard A. Ikeda*

Department of Chemistry and Biochemistry, Georgia Institute of Technology, Atlanta, Georgia 30332-0400

Received February 9, 1998; Revised Manuscript Received July 20, 1998

ABSTRACT: Human serum transferrin consists of two iron-binding lobes connected by a short peptide linker. While the high homology and structural similarity between the two halves of the molecule would suggest similar characteristics, it has been shown that the pH-dependent rate of release of iron from the N-terminal lobe is quite different from that of its C-terminal counterpart. This suggests that the N-lobe of human serum transferrin has a specific, pH-dependent, molecular mechanism for releasing iron. Sacchettini and co-workers using structural information have hypothesized that two lysines in the N-terminal lobe of ovotransferrin create a dilysine interaction and suggest that this is the trigger for pH-dependent iron release. To investigate this hypothesis, we used a *Pichia pastoris* expression system to produce large amounts of wild-type nTf, the single point mutants, nTfK206A (Lys 206 to alanine) and nTfK296A (Lys 296 to alanine), and the double mutant, nTfK206/296A. The purified recombinant proteins were then used to measure rates of iron release to pyrophosphate. It was found that the rate of iron release from all three mutant proteins at pH 5.7 (the pH at which nTf would normally release iron) was too slow to measure. Only when the pH was reduced to 5.0 could the rates of iron release from the mutant proteins be reliably determined. Although this precludes a direct comparison to wild-type nTf (the rate of iron release from nTf at pH 5.0 is too fast to measure), it implicates lysines 206 and 296 in the pH-dependent release of iron from nTf.

Serum transferrin, ovotransferrin, lactoferrin, and melanotransferrin are members of the highly homologous family of iron carrier glycoproteins (*1*−*3*). The structures of many transferrins have been solved, and they show that the proteins contain two lobes of about equal size connected by a short peptide linker (*4*−*8*). Each lobe can be further divided into two domains, which form a deep cleft and are joined by a flexible hinge. One iron binds per lobe in the cleft formed by the two domains. In holo-transferrin, the two domains are in the "closed" conformation, and in apo-transferrin, the two domains are in the "open" conformation. Although the two lobes are highly homologous, they have subtle differences in properties. The N-terminal lobe of human serum transferrin releases iron at ∼pH 5.7, while the C-terminal lobe retains iron until pH 4.8 (*9*−*11*). There are also differences in the iron-binding properties of different members of the transferrin family. Lactoferrin, for example, will retain its iron until pH 4 (*12*). Presumably the N-terminal lobe of human serum transferrin has a specific molecular mechanism for releasing iron at pH 5.7.

In the crystal structure of the iron-bearing, N-terminal lobe of hen ovotransferrin, Sacchettini and co-workers (*13*) found that the side-chain nitrogens of Lys 209 and Lys 301 are only 2.3 Å apart. These lysines are on different faces of the iron-binding cleft and are thought to be bridged by a single proton. This creates an "unusual interdomain interaction". Sacchettini (*13*) has hypothesized that above pH 6.0 the single bridging proton holds the N-lobe transferrin subdomains together. They also hypothesize that this dilysine motif is the trigger for pH-dependent Fe^{3+} release. They propose that at acid pH both lysines are protonated and that repulsion of the two positively charged lysines, which are located on opposite domains of the N-lobe, is the driving force that opens the two domains of ovotranferrin and facilitates release of Fe^{3+} by exposing the ion.

Lys 206 and Lys 296 in the N-terminal lobe of human serum transferrin are homologous to the trigger lysines of N-terminal hen ovotransferrin. In the crystal structure of monoferric human serum transferrin (*8*), the N-terminal lobe of human serum transferrin is open and lacks iron. As a consequence, an interdomain interaction of lysines 206 and 296 cannot be confirmed using structural data. Nonetheless, Sacchettini and co-workers suggest that lysines 206 and 296 form the pH trigger for the release of iron bound to the N-terminal lobe of human transferrin (*13*). If Sacchettini's proposed model is correct, then the protonation of the basic residues would explain why the N-terminal lobe of human serum transferrin releases iron at ∼pH 5.7, while the C-terminal lobe, which has a different set of amino acids and interactions at analogous positions, retains iron until pH 4.8.

† This work was supported by the National Science Foundation Grant MCB-9505824 and a Standard Grant in Aid from the Georgia Affiliate of the American Heart Association. S.K. was supported by a Georgia Tech/Howard Hughes Medical Institute Summer Research Fellowship for Undergraduate Students.

* To whom correspondence should be addressed. Phone: (404) 894-4037. Fax: (404) 894-7452. E-mail: rick.ikeda@chemistry.gatech.edu.

‡ Present address: TMB/DASTLR/NCID/CDC Mail Stop G35, 1600 Clifton Rd., NE, Atlanta, GA 30333.

S0006-2960(98)00318-3 CCC: $15.00
Published on Web 09/05/1998

Previous structure function studies with K206 and K296 have shown that nTfK206Q, which is based on the substitution in the C-terminal lobe of ovotransferrin, binds iron more tightly than does nTf[1] (*14*). Difference UV spectrophotometric studies on nTfK296Q and nTfK296E implicated this lysine as the proton binding site during the binding of synergistic and nonsynergistic anions (*15*). Iron release studies on the mutant K206R, which is based on the substitution in the N-terminal lobe of lactoferrin, show that nTfK206R releases iron more slowly to pyrophosphate than does nTf (*16*).

We have recently described the production of large amounts of nTf in the methylotropic yeast, *Pichia pastoris* (*17*). In the *Pichia* expression system, the gene of interest is cloned under the tightly controlled, methanol inducible alcohol oxidase promoter, P_{AOX1}, and is then integrated at the AOX1 locus by homologous recombination. The basic techniques required for the construction and growth of *Pichia* expression strains are similar to those used for *E. coli* and *S. cerevisiae* but offer additional benefits, including higher levels of expression, protein glycosylation, proteolytic maturation, and protein folding. We now report the use of a recently released modification of this system, which allows for the use of a His tag in the production and purification of site-directed mutants of nTf. The single mutants nTfK206A (lysine 206 to alanine) and nTfK296A (lysine 296 to alanine) and the double mutant nTfK206/296A were then used to further investigate the importance of lysines 206 and 296 in pH-dependent iron release from nTf.

MATERIALS AND METHODS

Construction of the Expression Plasmids. The point mutations were introduced into the nTf coding sequence by using the Altered Sites Mutagenesis Kit (Promega). In the *Pichia* expression plasmid pPIC9−nTf (*17*), the nTf coding sequence is flanked by the unique restriction sites *Xho*I and *Xba*I. These sites were used to transfer nTf from pPIC9−nTf to the same sites in pGEM−7Zf+ (Promega) to create the intermediate cloning plasmid pGEM−nTf. In this construct, the *Xho*I/*Xba*I nTf fragment is flanked by the restriction sites *Sma*I and *Xba*I. The *Sma*I/*Xba*I nTf fragment could then be transferred into the same sites of the mutagenesis cloning plasmid, pAlter, thus creating the plasmid pAlter−nTf. The point mutations were introduced into the nTf coding sequence using the reactions as described in the Altered Sites Mutagenesis Protocol (Promega). To create pAlter−nTfK206A, the primer 5′GTG GCC TTT GTC GCG CAC TCG ACT ATA TTT TTT ATA TCA GCT CAC GCG CTG TTT CCG GTG was used. To create pAlter−nTFK296A, the primer 5′AAG GAC CTG CTG TTT GCG GAC TCT GCC CAC GGG GGG CAC CCG TCT CAG GCG TTT GTC GTC CAG GAA was used. To create pAlter−nTfK206/296A both primers were used in the mutagenesis reaction. All mutations were confirmed by cycle sequencing (data not shown). The mutated nTf coding fragments (still flanked by *Xho*I and *Xba*I restriction sites) were then simply transferred back into the *pichia* expression plasmid, pPIC9, using the unique restriction sites *Xho*I and *Xba*I to create the plasmids pPIC9−nTfK206A, pPIC9−nTfK296A, and pPIC9−nTfK206/296A (Figure 1). These expression plasmids were capable of producing the mutant proteins (data not shown); however, a second *Pichia* expression plasmid, pPICZαB, was chosen for these studies because it allowed for easier purification of the mutant proteins.

The expression plasmid pPICZαB differs from the *Pichia* expression plasmid used in previous work (*17*) in that it replaces both the ampicillin resistance gene (for selection in *E. coli*) and the HIS4 gene (for selection in His$^-$ *P. pastoris*) with the zeocin antibiotic resistance gene, *Sh ble*. The plasmid also contains sequences coding for a hexahistidine tag downstream of the polylinker, which allows for a simple one-step purification of recombinant fusion protein on a nickel affinity column. A fragment coding for nTfK206A (amino acids 1−338) was amplified from pPIC9−nTfK206A using primers [Tf-N(*Pml*I), 5′ATG ACT CAC GTG GTC CCT GAT AAA ACT GTG, and nTf-C(*Acc*I), 5′ATG ACT GTC GAC TTC TGG GCA TGT GCC TTC] designed to fuse the 5′ end of the gene to a *Pml*I restriction site, to eliminate the stop codon at amino acid 339 and to fuse the 3′ end of the gene to an *Acc*I restriction site. This fragment was then inserted into the *Pml*I and *Acc*I sites in pPICZαB, fusing the 5′ end of nTfK206A in frame to the *S. cerevisiae* prepro α signal sequence and the 3′ end to the His tag sequence, thus creating the plasmid, pPICZαB−nTfK206A (Note: The use of the *AccI* restriction site deletes the myc epitope of pPICZαB). To create the expression plasmids pPICZαB−nTf, pPICZαB−nTfK296A, and pPICZαB−nTfK206/296A, the unique restriction sites *Bsp*E1 and *Nde*I within the nTfK206A coding sequence were used. These enzymes cut near the ends of the nTfK206A fragment but do not cut the pPICZαB vector, allowing the simple replacement of the *Nde*I/*Bsp*E1 nTfK206A fragment with the *Nde*I/*Bsp*EI fragments of nTf, nTfK296A, or nTfK206/296A. pPICZαB−nTfK206A was digested with *Nde*I and *Bsp*EI, and the vector fragment was isolated and purified. pPIC9nTf, pPIC9−nTfK296A and pPIC9−nTfK206/296A were digested with *Bsp*EI and *Nde*I; the respective nTf *Nde*I/*Bsp*EI fragments were isolated and ligated to the purified vector, thus creating pPICZαB−nTf, pPICZαB−nTfK296A, and pPICZαB−nTfK206/296A (Figure 1). All plasmids were confirmed by sequencing (data not shown).

Construction of the Pichia Expression Strains. pPICZαB was designed to only be linearized in the 5′ AOX1 region, which limits recombination to single crossover events and inserts the entire expression vector at the AOX1 locus next to a fully intact AOX1 gene. The *P. pastoris* strain, KM71, which was used in these studies, contains a point mutation in the AOX1 gene, yielding a strain with a Mut^S (methanol utilization sensitive) phenotype. This was desired because the expression and production profile of nTf in a Mut^S strain had already been well-characterized by the authors in preliminary studies (data not shown). *Pichia* expression strains were constructed as described in the Pichia Expression System users manual (Invitrogen). Electrocompetent KM71 were incubated with 0.02 mg of expression plasmid DNA

[1] Abbreviations: AOX, alcohol oxidase; apo-transferrin, transferrin without iron; BMGY, buffered glycerol complex medium; BMMY, buffered methanol complex medium; histidine tag, fusion peptide containing six consecutive histidines; holo-transferrin, transferrin containing iron; Mut$^+$, wild-type methanol utilization phenotype; Mut^S, sensitive methanol utilization phenotype; n-rabTf, N-terminal lobe of rabbit serum transferrin; n-ovoTf, N-terminal lobe of hen ovotransferrin; nTf, recombinant N-terminal lobe of human serum transferrin; YPDS, yeast peptone dextrose medium.

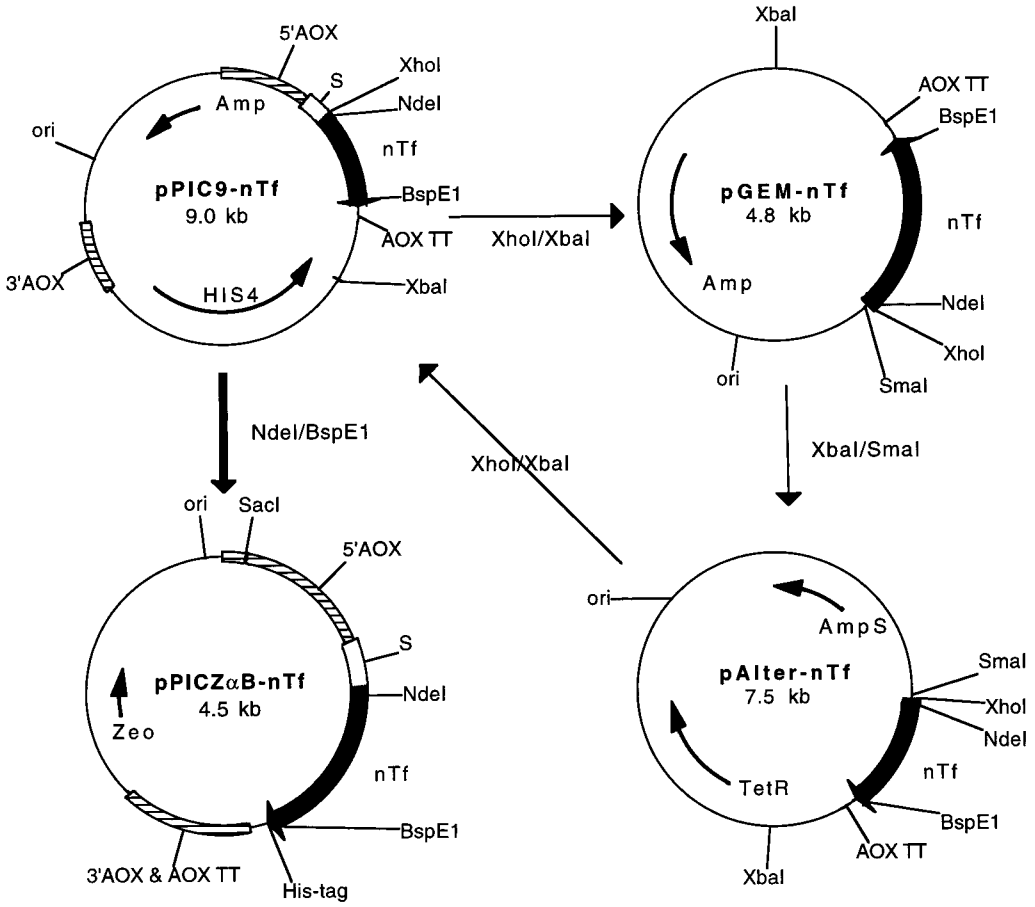

FIGURE 1: Construction of *Pichia pastoris* nTf expression vectors. The plasmid pPIC9−nTf has been described by Steinlein et al. (*17*). pGEM−7Zf+ was used to shuttle nTf between pPIC9−nTf and pAlter. pAlter−nTf was used for site-directed mutagenesis to create pAlter−nTfK206A, pAlter−nTfK296A, and pAlter−nTfK206/296A. The plasmid pPICZαB−nTfK206A was created by PCR-based amplification of pPIC9−nTfK206A as described in Materials and Methods. The plasmids pPICZαB−nTf, pPICZαB−nTfK296A, and pPICZαB−nTfK206/296A were created by replacing the *Nde*I/*Bsp*EI fragment in pPICZαB−nTfK206A with the appropriate fragment from pPIC9−nTf(wt/mut). 5′AOX, 5′AOX1 region for homologous recombination and the AOX1 promoter; S, α-factor signal sequence; nTf, nTf coding sequence; TT, AOX1 transcription terminator; HIS4, HIS4 gene for selection in *His*$^-$ *P. pastoris*; 3′AOX, 3′AOX1 region for homologous recombination; ori, *E. coli* origin; Amp, ampicillin resistance gene, Amp^S, ampicillin resistance gene containing a point mutation; Tet, tetracycline resistance gene; Zeo, Zeocin resistance gene.

linearized with *Sac*I for 10 minutes on ice and then electroporated using the Invitrogen Electroporator II with a charging voltage of 1500 V, a capacitance of 50 μF, and a resistance of 200 Ω in a 0.2 cm cuvette. The transformed cells were resuspended in 1 mL ice-cold 1 M sorbitol, incubated at 30 °C for 2 h, and then plated on YPDS plates (1% yeast extract, 2% peptone, 2% dextrose, 1.0M sorbitol) containing zeocin (Note: 0.5 mg/mL zeocin was used to select for transformants containing multiple copies of the zeocin antibiotic resistance gene. These transformants are also likely to contain multiple copies of the entire expression plasmid and may improve protein expression.). Zeocin-resistant transformants were used to innoculate 2 mL BMGY (1% yeast extract, 2% peptone, 100 mM potassium phosphate, 1.34% yeast nitrogen base, 0.4 μg/mL biotin, 1% glycerol), and the culture was grown at 30 °C to an OD_{600} equivalent to 15. At this point, the cells were collected by centrifugation and resuspended in 0.5 mL BMMY (1% yeast extract, 2% peptone, 100 mM potassium phosphate, 1.34% yeast nitrogen base, 0.4 μg/mL biotin, 0.5% methanol), which contains methanol to induce the AOX1 promoter. After 48 h of induction, the cells were harvested by centrifugation. Samples of the harvested culture medium were analyzed by SDS−PAGE on 14% acrylamide (29:1 crosslink) gels (*18*), followed by staining with Coomassie blue (Figure 2). The SDS−PAGE gel visualized by Coomassie showed that KM71[pPICZαB−nTf], KM71[pPICZαB−nTfK206A], KM71-[pPICZαB−nTfK296A], and KM71[pPICZαB−nTfK206/296A] produce large amounts of an nTf protein. One strain of each with a high level of protein production (as determined by gel electrophoresis only) was chosen for further study. Genomic DNA from each strain selected for protein purification was isolated using the Easy DNA Kit (Invitrogen), and all mutations were again confirmed by cycle sequencing.

Production and Purification of Recombinant Protein. To produce large amounts of each nTf protein, 200 mL of KM71[pPICZαB−nTf(wild-type/mutant)] were grown at 30 °C to an OD_{600} equivalent to 15−20 in BMGY. The cells were harvested by centrifugation, resuspended in 20 mL BMMY, and grown for an additional 68 h. The yeast were then removed from the culture by centrifugation, and the cleared media was concentrated to 3 mL in a Centriplus-10 (Amicon). The cleared media was diluted 1:8 with binding buffer (20 mM sodium phosphate, pH 7.8, 500 mM NaCl) plus 1 mM PMSF and loaded onto a 1 mL His-Bind resin column that had been charged with 50 mM $NiSO_4$ and equilibrated with binding buffer. The column was washed with 10 mL of binding buffer, and the protein was eluted

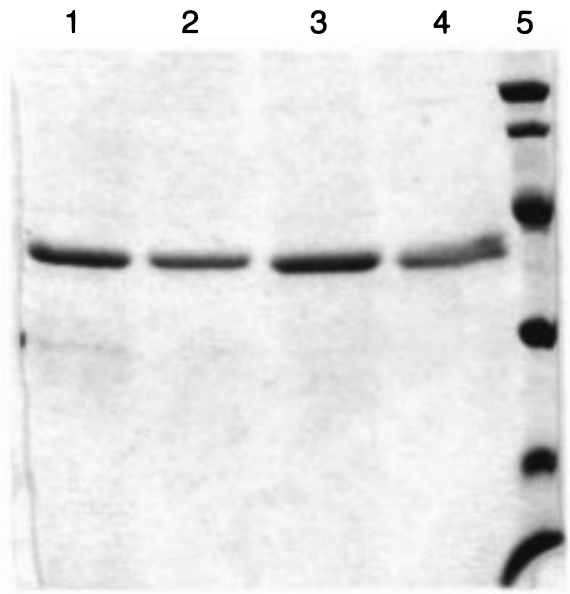

FIGURE 2: Expression of nTf and nTf mutants from KM71-[pPICZαB−nTf(wt/mut)]. SDS−PAGE analysis of induced cell culture supernatants. Lane 1: KM71[pPICZαB−nTf)]. Lane 2: KM71[pPICZαB−nTfK206A]. Lane 3: KM71[pPICZαB−nTfK296A]. Lane 4: KM71[pPICZαB−nTfK206/296A]. Lane 5: molecular weight makers (97.4, 66.2, 45, 31, 21.5, and 14.4 kDa).

with 9 mL of elution buffer (20 mM sodium phosphate (pH 7.8), 500 mM NaCl, 1 M imidazole). The eluted sample was concentrated in a Centricon-10 (Amicon), and the buffer was changed three times during the concentration process by diluting 0.5 mL of sample to 20 mL with 50 mM Tris-HCl, pH 8.4 plus 5 mM sodium bicarbonate. The protein concentration was determined by Bradford assay (BioRad) and analyzed for purity by SDS−PAGE. Iron was added to the protein by the addition of 5 mM Fe−NTA to a saturation of 150%.

If apo-protein was needed, iron was removed from the sample by the addition of 0.1 vol of 0.5 M NaOAc (pH 5), 1 mM EDTA, and 1 mM NTA followed by 0.03 vol 1.3 N HCl.

Iron-Binding Analysis. Urea−PAGE gels (7 cm × 8.5 cm minigel apparatus) were 6% acrylamide (39:1 crosslink) containing 6 M urea in 1X TBE. The gel was loaded with 3−10 μg of each sample and run at 200 V for 1.25 h (*19*−*21*). Visible absorption spectra were recorded on a Shimadzu UV-160 spectrophotometer. The apo-protein was made 5−15 mg/mL in 50 mM Tris-HCl, pH 8.4, 5 mM bicarbonate and titrated with 5 mM Fe(NTA) while monitoring the absorbance at 465 nm using apo-protein solution as the reference (*20*).

Iron-Release Analysis. The kinetics of iron release were followed by using a spectrofluorometric assay developed by Egan et al. (*22*) using conditions later modified by Zak et al. (*16*). The recombinant proteins were made 100 nM in 100 mM MES at a range of pH values (pH 5.0−6.5) plus either 100 or 600 mM NaCl. Data accumulation was initiated upon the addition of 0.05−25 mM pyrophosphate to the protein solution, and fluoresence intensity was recorded as a function of time. A Shimadzu RF5301 spectrofluorimeter was used.

Calculation of Cation-π Angles and Distances. Crystallographic coordinates for the structures of n-rabTf (1TFD, ref *6*) and n-ovoTf (1NNT, ref *13*) were obtained from the Protein Data Bank. The distances from lysines 206 and 296 or lysines 209 and 301 to the centroid of each of the neigboring aromatic amino acids and the angles created by a line from a lysine to the centroid and a line normal to the ring of an aromatic amino acid were calculated with standard formulas from analytic geometry (*23*).

Rectangular coordinates for the centroids of the rings of the aromatic residues listed in Tables 1 and 2 were determined by averaging the *X*, *Y*, and *Z* coordinates of the ring atoms. The direction numbers (*a*, *b*, and *c*) and the lengths of the lines connecting the centroids of the aromatic rings and the ϵ carbons or the amino nitrogens of the lysines (as listed in Tables 1 and 2) were calculated with eqs 1 and 2 (*23*),

$$a = x_1 - x_2; \quad b = y_1 - y_2; \quad c = z_1 - z_2 \tag{1}$$

$$\text{distance} = (a^2 + b^2 + c^2)^{1/2} \tag{2}$$

where x_1, y_1, and z_1 are the coordinates of the centroid and x_2, y_2, and z_2 are the coordinates of the ϵ carbon or the amino nitrogen.

Direction numbers (a_n, b_n, and c_n) for lines normal to the planes of the rings of the aromatic amino acids were calculated with eqs 3, 4, and 5 (23)

$$a_n = (y_2 - y_1)(z_3 - z_1) - (z_2 - z_1)(y_3 - y_1) \tag{3}$$

$$b_n = (z_2 - z_1)(x_3 - x_1) - (x_2 - x_1)(z_3 - z_1) \tag{4}$$

$$c_n = (x_2 - x_1)(y_3 - y_1) - (y_2 - y_1)(x_3 - x_1) \tag{5}$$

where x_{1-3}, y_{1-3}, and z_{1-3} are the coordinates of three atoms in the aromatic ring of an amino acid. The angles between the line from an ϵ carbon or an amino nitrogen of the lysines listed in Tables 1 and 2 to the centroid of the ring of a neigboring aromatic residue and the line normal to the plane of the ring of the aromatic residue were then calculated with eq 6 (*23*),

$$\cos\theta = \frac{(a)(a_n) + (b)(b_n) + (c)(c_n)}{(a^2 + b^2 + c^2)^{1/2}(a_n^2 + b_n^2 + c_n^2)^{1/2}} \tag{6}$$

where θ is the angle between the lines.

RESULTS AND DISCUSSION

The results presented here demonstrate that a *Pichia pastoris* expression vector encoding a zeocin resistance marker and an affinity fusion peptide can be used for the rapid production and purification of large amounts of nTf and nTf mutants. The use of zeocin as the selection marker on the vector greatly simplified the isolation of *Pichia* strains containing the nTf expression clones. The vector also allowed for the expression of recombinant nTf proteins that are fused to a hexahistidine peptide (histidine tag), and the histidine tag allowed for rapid purification of recombinant nTf proteins. In addition, there was no obvious difference in the expression levels of the mutant and wild-type nTf proteins (80−100 mg/L of cell culture) in *Pichia pastoris*, as has been reported for the expression of nTf mutants in baby hamster kidney cells (*14*). It also appeared that the

Table 1: Analysis of Cation Pi Interactions in the N-terminal Lobe of Chicken Ovotransferrin

	Lys 209				Lys 301			
	amino N		CH_2		amino N		CH_2	
	dist (Å)	angle (deg)	dist (Å)	angle (deg)	dist (Å)	angle (deg)	dist (Å)	angle (deg)
Tyr 82	3.8	14.4	5.2	11.5	4.2	41.0	4.8	50.5
Tyr 92	4.1	34.3	4.6	44.9	3.5	4.2	4.9	2.9
Tyr 191	5.5	28.3	5.2	20.2	4.6	50.2	4.2	49.3
His 250	6.7	21.9	7.6	27.2	4.5	20.9	4.5	10.9

Table 2: Analysis of Cation Pi Interactions in the N-terminal Lobe of Rabbit Serum Transferrin

	Lys 206				Lys 296			
	amino N		CH_2		amino N		CH_2	
	dist (Å)	angle (deg)	dist (Å)	angle (deg)	dist (Å)	angle (deg)	dist (Å)	angle (deg)
Tyr 85	4.2	20.3	5.2	7.8	4.0	38.1	4.1	58.0
Tyr 95	4.4	32.4	3.7	34.5	3.7	21.9	5.0	30.2
Tyr 188	6.5	34.6	5.8	29.9	5.1	61.3	5.5	71.1
His 249	7.4	20.3	7.4	28.5	4.5	16.2	4.1	7.3

C-terminal histidine fusion tag did not interfere with the binding of iron by nTf. Titration of 100 μL of a 12.8 mg/mL solution of apo-nTf bearing a C-terminal histidine tag in 50 mM Tris-HCl, pH 8.4, 1 mM sodium bicarbonate buffer with Fe−NTA yielded a ϵ_{465}(mM) of 2.1, which is in excellent agreement with previously reported values (*20*).

In this study, we have created the mutants nTfK206A, nTfK296A, and the double mutant nTfK206/296A to investigate the role of lysines 206 and 296 in pH-dependent iron release. If Sacchettini's hypothesis is true, then the substitution of an alanine for Lys 206 and/or Lys 296 should destroy pH-dependent iron release by N-terminal half-transferrin. Alternatively, if these residues are not involved in the pH-dependent release of iron, then the mutant half-transferrin should bind and release iron naturally. The ability of the recombinant mutant nTf's to bind and release iron was measured by a gel shift mobility assay. This assay, which was first described by Mackey and Seal (*19*) and later modified by others (*20*, *21*), allows for the separation of holo-transferrin from apo-transferrin on a urea polyacrylamide gel. The iron-free form of transferrin denatures in the urea concentration used, and its mobility in the gel decreases. In contrast, the iron-loaded form is not denatured and its mobility in the gel is not affected (Figure 3). Iron-loaded nTf, nTfK206A, nTfK296A, and nTfK206/296A were incubated in 100 mM NaOAc, 0.1 mM EDTA, 0.1 mM NTA at pH 3.6, 4.2, 5.0, 5.6, and 8.4 at 37 °C for 5 h, and their iron status was measured by urea−PAGE analysis (Figure 3). All of the nTf proteins retained iron at pH 8.4, and nTf was in the apo-form at pH 5.6 as expected. The mutants nTfK206A, nTfK296A, and nTfK206/296A displayed less pH sensitivity than the wild-type and remained in the iron-loaded form at pH 5.6. At pH 5.0, the double mutant nTfK206/296A was in the apo-form, while the single mutants nTfK206A and nTfK296A appeared to partially retain iron. As discussed in the next paragraph, iron release by nTfK206A and nTfK296A at pH 5.0 is very slow. Given the relatively low concentration of iron chelators in the nTfK206A and nTfK296A samples and the length of time these samples were incubated before electrophoresis, it is very likely that the single mutants had not reached equilibrium at pH 5.0; consequently, ferric nTfK206A and ferric nTfK296A were still present in the samples. At pH 4.2 and pH 3.6 the nTfK206A and nTfK296A mutants were observed in their apo-forms.

To further investigate the iron release characteristics of the mutant nTf proteins, the rates of iron release from the proteins were measured using a spectrofluorometric assay (*22*). The effect of pH on the iron release rates was considered first, and the results are tabulated in Table 3. Using this assay, we could reliably measure observed rates of iron release as slow as 0.01 min^{-1} to as fast as 10 min^{-1}. The rate of iron release from nTf could only be measured at a pH $\geq$ 5.7; unfortunately, the rates of iron release from the mutant proteins could only be measured at a pH $\leq$ 5.2 (double mutant) and a pH $\leq$ 5.0 (single mutants). This precluded a direct comparison of observed iron release rates under identical conditions, but it did allow a qualitative comparison to be made. At pH 6.5 and 5.7, only the rate of iron release from nTf could be measured (k_{obs} of 2.64 and 11.4 min^{-1}, respectively, and half-lives of 0.263 and 0.061 min, respectively); the rates of iron release from the mutant nTf proteins were too slow to be measured. This indicates that at pH 6.5 and 5.7, the mutant nTf proteins had rates of iron release that were at least 250−1000 times slower than those of wild-type nTf. At pH 5.0, the rate of iron release from the double mutant was 0.172 min^{-1} (4.0 min half-life) and the rates of iron release from the single mutants nTfK206A and nTfK296A were 0.018 (38.5 min half-life) and 0.010 min^{-1} (69.3 min half-life) respectively; however, at this pH, the rate of iron release from nTf was too fast to measure. This indicated that the mutant proteins were releasing iron at rates that were at least 100−1000 times slower than that of the wild-type. Interestingly, the single mutants released iron at a rate that is an order of magnitude slower than that of the double mutant. This difference in release rates may be due to lysine cation π interactions that remained in the single mutants, but were absent in the double mutant.

In Sacchettini's analysis of the structure of the monoferric N-terminal lobe of hen ovotransferrin (n-ovoTf) (*13*), the investigators proposed that lysines 209 and 301 (the hen n-ovoTf residues equivalent to Lys 206 and 296 of human nTf) interacted with each other and with neighboring

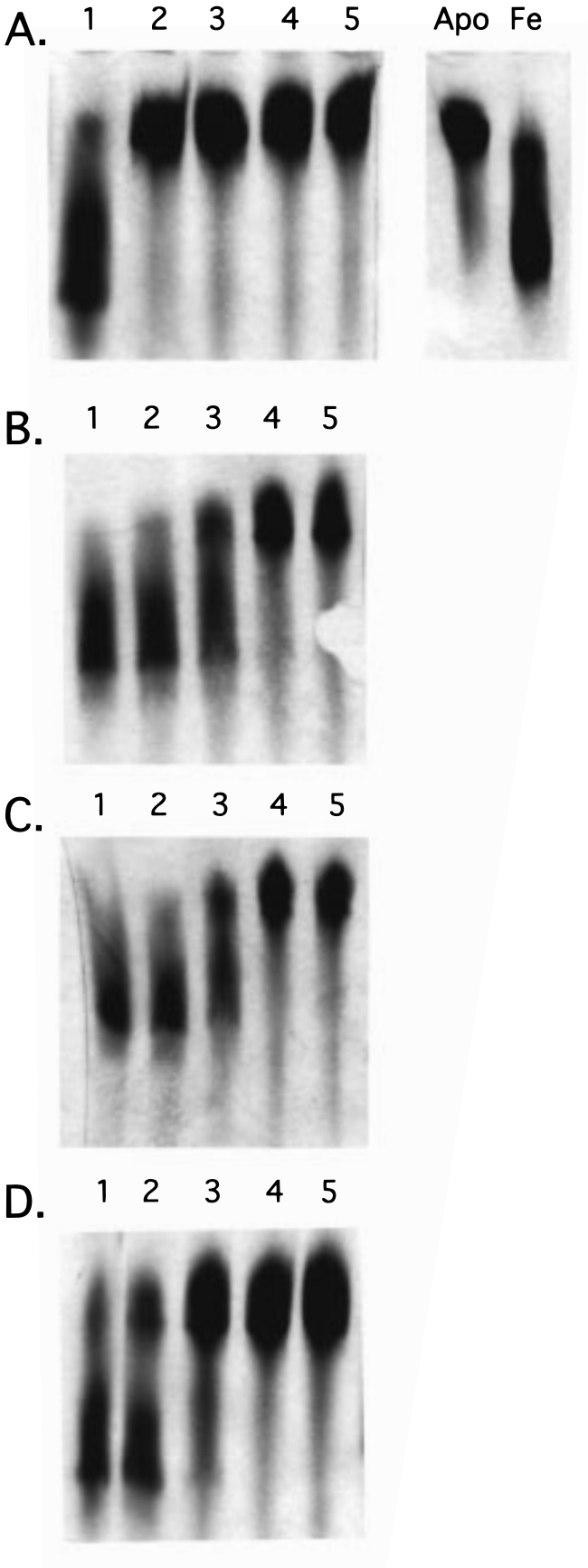

FIGURE 3: Recombinant nTf and nTf mutants bind and release iron. Urea−PAGE analysis. (A) nTf (3 μg), apohuman serum transferrin (10 μg) (lane apo) and Fe human serum transferrin (10 μg) (lane Fe), (B) nTfK206A (3 μg), (C) nTfK296A (3 μg), and (D) nTfK206/296A (3 μg) incubated at pH 8.4 (lane 1), pH 5.6 (lane 2), pH 5.0 (lane 3), pH 4.2 (lane 4), and pH 3.6 (lane 5).

Table 3: Rates of Iron Release[a] (k_{obs}(min^{-1}))

sample	pH 6.5	pH 5.7	pH 5.2	pH 5.0
nTf	2.64 ± 0.34	11.4 ± 3.8	too fast[c]	too fast[c]
K206/296AA	too slow[b]	too slow[b]	0.087 ± 0.020	0.172 ± 0.020
K206A	too slow[b]	too slow[b]	too slow[b]	0.018 ± 0.002
K296A	too slow[b]	too slow[b]	too slow[b]	0.010 ± 0.002

[a] Iron release from recombinant nTf to 500 μM pyrophosphate. The samples contained 100 nM protein, 100 mM MES (at the pH values listed in the table), and 100 mM NaCl. [b] k_{obs} was too fast to be reliably determined with this assay. [c] k_{obs} was too slow to be reliably determined with this assay.

aromatic residues. Specifically, the interaction of Lys 209 and 301 with each other formed the dilysine motif that in its monoprotonated form holds the two domains of n-ovoTf closed and in its diprotonated form forces the two domains of n-ovoTf apart, while the interaction of Lys 209 and 301 with Tyr 82 and 92, respectively, formed amino−aromatic hydrogen bonds (*13*).

A recent reevaluation of the interactions of protonated lysines with the π orbitals in the faces of the rings of aromatic amino acids now redefines these interactions as electrostatic cation π interactions (*24*−*26*). Cation π interactions are noncovalent electrostatic interactions between a cation and electron-rich π orbitals. The interaction was first recognized in the gas phase, but recent work by Dougherty and co-workers with artificial cyclophane receptors has demonstrated that cation π interactions in aqueous media are as important as hydrogen bonding, ion pairs, and hydrophobic interactions. In cyclophanes, a single cation π interaction is estimated to be worth ~0.5 kcals (*24*, *26*).

In the case of proteins, Burley and Petsko (*27*) noted in 1986 that a large proportion of NH groups on amino acid side chains are found in close contact (less than 6 Å) with aromatic side chains in high-resolution crystal structures. This observation was confirmed by Thornton and co-workers (*28*) in 1990, and more recently, the associations of cations with an aromatic rings in acetyl choline esterase, acetyl choline receptors, alkylamine dehydrogenases, and ion channels have been described as potential cation π interactions (*24*, *26*). However, the strength of a cation π interaction in a protein has only been measured in barnase. In barnase, a His^+−Trp cation π interaction is worth 1.4 kcals relative to solvation in water (*29*).

In the crystal structure of monoferric n-ovoTf, Lys 209 and 301 sit in a pocket formed by the aromatic amino acids Tyr 82, Tyr 92, Tyr 191, and His 250 (*13*), and an analogous arrangement is found in the crystal structure of the monoferric N-terminal lobe of rabbit transferrin (n-rabTf). The two lysines (Lys 206 and 296) that form the dilysine motif of n-rabTf sit in a pocket that is formed by the aromatic amino acids Tyr 85, Tyr 95, Tyr 188, and His 249 (*6*). In both n-ovoTf and n-rabTf, the second and third tyrosines and the histidine are also ligands for the bound Fe^{3+} ion. Since human nTf is more closely related to n-rabTf and the residue numbering of nTf is more like that of n-rabTf, the dilysine motif, the aromatic amino acid pocket (π pocket), and the bound iron of n-rabTf are shown in Figure 4.

Dougherty has found that cation π interactions exhibit a $1/r^n$ dependence, where $n < 2$ (*24*), and believes that since the cation π interaction is essentially a charge interaction and not a special kind of "bond", the dependence of cation

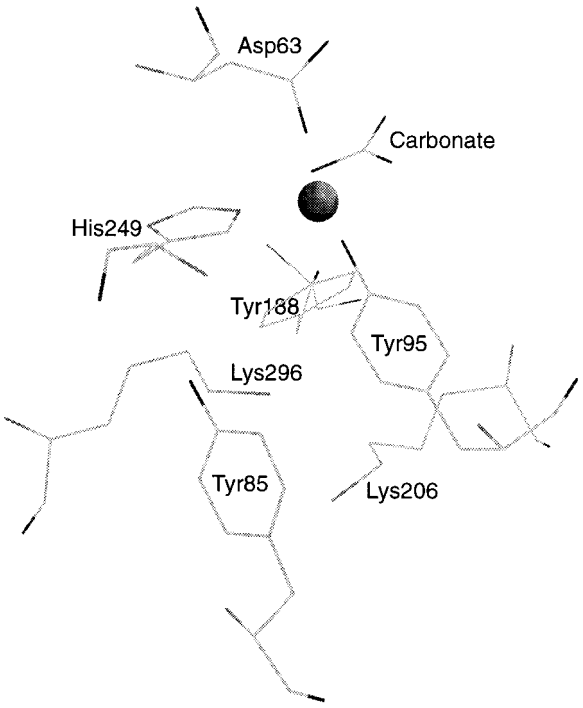

FIGURE 4: Iron binding site and the lysine trigger in the N-terminal lobe of rabbit serum transferrin as seen in the crystal structure (*6*).

π interactions on the angular position of the cation in relation to the π orbitals should not be severe, as long as the cation is more strongly associated with the face and not the edge of the π system (*30*). It has also been shown that lysine cation π interactions can occur through both the protonated side chain amino group and the CH_2 directly adjacent to the charged amine, since a CH_2 directly adjacent to a positively charged group carries substantial positive character (*24*, *26*).

Distances from the protonated nitrogen atoms of the lysines to the centroid of each of the neighboring aromatic amino acids and the angles created by a line from the nitrogens to the centroid and perpendicular lines through the centroids of the aromatic amino acids were calculated for n-ovoTf and n-rabTf. The same measurements were also calculated for the ϵ carbons of the lysines, and the data is presented in Tables 1 and 2.

At present, there are insufficient examples of cation π distances and geometries in proteins to specify typical distances and angles between the cation and the π orbitals of a protein cation π interaction, but the distance and angular dependencies cited by Dougherty (*24*, *30*) suggest that the dilysine residues could potentially interact with all of the neighboring aromatic residues. Nevertheless, some of these cation π interactions would be more favorable than others. In n-ovoTf, Lys 209 would be expected to interact most favorably with Tyr 82, Tyr 92, and Tyr 191, and Lys 301 would be expected to interact most favorably with Tyr 82, Tyr 92, and His 250; while in n-rabTf, Lys 206 would be expected to interact most favorably with Tyr 85, Tyr 95, and Tyr 188, and Lys 296 would be expected to interact most favorably with Tyr 85, Tyr 95, and His 249.

Cation π interactions are known to stabilize the protonation of basic residues (*24*, *26*, *29*); consequently, the pK_as of the dilysine residues of n-ovoTf and n-rabTf should increase, but since the interactions of both lysines with the surrounding π pocket are similar, the pK_as of the lysines should be affected equally. This would leave the dilysine residues with relatively similar pK_as and would preserve the ability of the two lysines to share a single proton. In the ferric forms of n-ovoTf and n-rabTf, cation π interactions would provide additional interdomain interactions that could help hold the two domains of n-ovoTf and n-rabTf closed. Finally, cation π interactions with Tyr 92 and Tyr 191 in n-ovoTf and Tyr 95 and Tyr 191 in n-rabTf may make these tyrosines more acidic and help stabilize the phenolate ligands that bind Fe^{3+} ion.

Since the N-terminal lobe of human transferrin does not contain iron in the crystal structure (*8*), cation π interactions in the N-lobe of human transferrin cannot be verified; however, the structure of human transferrin is similar to rabbit transferrin, and we believe cation π interactions in the N-lobe of human transferrin will be qualitatively equivalent to the cation π interactions in n-rabTf. These cation π interactions may explain why the nTf single mutants nTfK206A and nTfK296A released iron more slowly than the nTf double mutant, nTfK206/296A. In the single mutants, the removal of one lysine would destroy the dilysine motif but would leave a lysine that can participate in cation π interactions and help hold the two domains of the mutants closed. In the double mutant, the removal of both lysines would destroy the dilysine motif and would destroy cation π interactions in the π pocket. Destruction of the cation π interactions would remove the interdomain interactions that they contribute and would accelerate the rate of iron release.

A second hypothesis regarding the release of iron from the N-terminal domain of human serum transferrin also involves lysines 206 and 296. Zucolla (ref *8*, personal communication) has noted that pyrophosphate, which is known to cause transferrin to release its iron, will just fit between lysines 206 and 296 in the crystal structure of the open N-terminal lobe of monoferric transferrin. Zucolla proposed that this is the binding site for pyrophosphate and the binding of pyrophosphate between these lysines opens the iron-binding cleft and releases iron. If Zucolla's hypothesis is true, then the substitution of alanines in place of lysines 206 and 296 should eliminate the pyrophosphate binding site in nTf and eliminate pyrophosphate-dependent iron release. If the binding of pyrophosphate to Lys 206 and Lys 296 is not involved in pyrophosphate dependent iron release, then the alanine mutants should still release iron in a pyrophosphate-dependent manner.

To determine if lysines 206 and 296 are part of the hypothesized pyrophosphate binding site, the rates of iron release from the mutant nTf proteins were measured at pH 5.0 and at pyrophosphate concentrations ranging from 50 μM to 25 mM (Figure 5). Iron release rates for all of the nTf mutants increased with increasing pyrophosphate concentration up to saturating conditions of approximately 20 mM. This suggested that lysines 206 and 296 are not important binding sites for pyrophosphate during iron release.

Finally, to investigate if Lys 206 and 296 are part of a secondary anion binding site described by Zak et al. (*16*), the effect of $[Cl^-]$ on the rate of iron release from nTfK206/296A was evaluated. The rate of iron release from the double mutant to 0.5 mM pyrophosphate was measured at pH 5.0 and NaCl concentrations ranging from 0.1 to 0.6 M (Figure 6). It was found that release rates decreased with increasing NaCl concentrations. These data mirror the

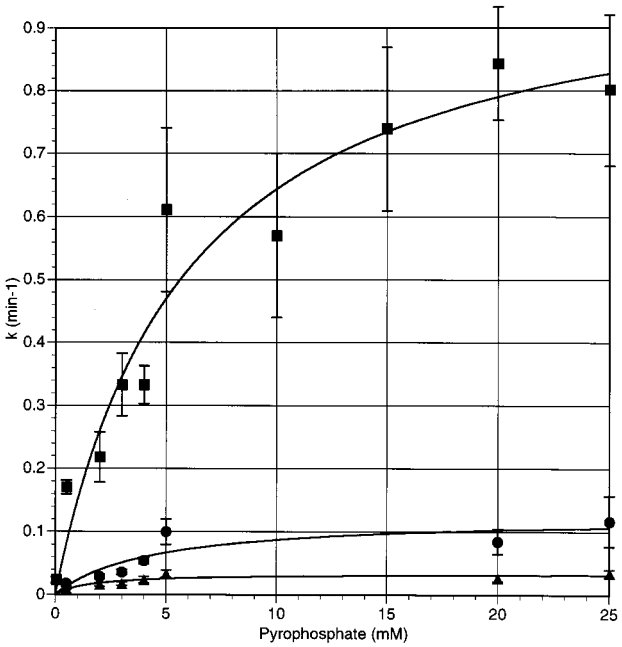

FIGURE 5: Dependence of the rate of iron release on the concentration of pyrophosphate. The rates of iron release to pyrophosphate from the mutant proteins at pH 5.0 were measured at pyrophosphate concentrations ranging from 50 μM to 25 mM. The proteins were 100 nM in 100 mM MES (pH 5.0) and 100 mM NaCl. The data points shown on the graph represent the average of three independent measurements nTfK206A/296A (B), nTfK206A (J), and nTfK296A (H).

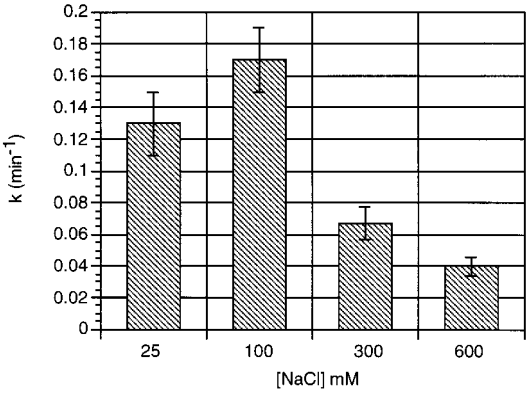

FIGURE 6: Iron release from nTfK206/296A is affected by NaCl concentrations. The rates of iron release to pyrophosphate from nTfK206/296A at pH 5.0 were measured at NaCl concentrations ranging from 25 mM to 0.6 M. The samples contained 100 nM protein in 100 mM MES (pH 5.0) and 0.5 mM pyrophosphate.

inhibitory effect of Cl^- on the rate of iron release from nTf as reported by Zak et al. (*16*) and suggest that lysines 206 and 296 are not involved in the proposed secondary N-terminal anion binding site.

In conclusion, we have shown that large amounts of nTf and nTf mutants can be expressed in *Pichia pastoris* and that the recombinant proteins can be quickly and easily purified by affinity chromatography when the nTf proteins are fused to a C-terminal histidine tag. Characterization of the mutant proteins produced in this study provided experimental support for the hypothesis that lysines 206 and 296 form the trigger for pH-dependent iron release from nTf and also provided evidence that lysines 206 and 296 are not part of nTf binding sites for pyrophosphate or chloride.

ACKNOWLEDGMENT

We would like to thank Dr. Dennis A. Dougherty, California Institute of Technology, for reading the manuscript and providing insightful comments.

REFERENCES

1. Powell, M. J., and Ogden, J. E. (1990) *Nuc. Acids. Res. 18*, 4013.
2. Rose, T. M., Plowman, G. D., Teplow, D. P., Dreyer, W. J., Hellstrom, K. E., and Brown, T. P. (1986) *Proc. Natl. Acad. Sci. USA 83*, 1261−1265.
3. Yang, F., Lum, J. B., McGill, J. R., Moore, C. M., Naylor, S. L., van Bragt, P. H., Baldwin, W. D., and Bowman, B. H. (1984) *Proc. Natl. Acad. Sci. U SA 81*, 2752−2756.
4. Anderson, B. F., Baker, H. M., Norris, G. E., Rice, D. W., and Baker, E. N. (1989) *J. Mol. Biol. 209*, 711−734.
5. Anderson, B. F., Baker, H. M., Norris, G. E., Rumball, S. V., and Baker, E. N. (1990) *Nature 344*, 784−787.
6. Bailey, S., Evans, R., Garrat, R. C., Gorinsky, B., Hasnain, S., Horsburgh, C., Jhoti, H., Lindley, P., Mydin, A., Sarra, R., and Watson, J. L. (1988) *Biochemistry 27*, 5804−5812.
7. Sarra, R., Garratt, R., Gorinsky, B., Jhoti, H., and Lindley, P. (1990) *Acta Crystallogr. B46*, 763−771.
8. Zuccola, H. J. (1992) *The crystal structure of monoferric human serum transferrin* Ph.D. Thesis, Georgia Institute of Technology, Atlanta, GA.
9. Evans, R. W., and Williams, J. (1978) *Biochem. J. 173*, 543−552.
10. Lestas, A. N. (1976) *Br. J. Haematol. 32*, 341−350.
11. Princiotto, J. V., and Zapolski, E. J. (1975) *Nature 255*, 87−88.
12. Montreuil, J., Tonnelat, J., and Mullet, S. (1960) *Biochim. Biophys. Acta 45*, 413−421.
13. Dewan, J. C., Mikami, B., Hirose, M., and Sacchettini, J. C. (1993) *Biochemistry 32*, 11963−11968.
14. Woodworth, R. C., Mason, A. B., Funk, W. D., and MacGillivray, R. T. A. (1991) *Biochemistry 30*, 10824−10829.
15. Cheng, Y., Mason, A. B., and Woodworth, R. C. (1995) *Biochemistry 34*, 14879−14884.
16. Zak, O., Aisen, P., Crawley, J. B., Joannou, C. L., Kokila, J. P., Rafiqu, M., and Evans, R. W. (1995) *Biochemistry 34*, 14428−14434.
17. Steinlein, L. M., Graf, T. N., and Ikeda, R. A. (1995) *Protein Expression Purif. 6*, 619−624.
18. Garfin, D. E. (1990) *Methods Enzymol. 182*, 425−441.
19. Mackey, D. G. and Seal, U. S. (1976) *Biochim. Biophys. Acta 453*, 250−256.
20. Funk, W. D., MacGillivray, R. T. A., Mason, A. B., Brown, S. A., and Woodworth, R. C. (1990) *Biochemistry 29*, 1654−1660.
21. Hirose, M., Akuta, T., and Takahashi, N. (1989) *J. Biol. Chem. 264*, 16867−16872.
22. Egan, T. J., Zak, O., and Aisen, P. (1993) *Biochemistry 32*, 8162−8167.
23. McLenaghan, R., and Levy, S. (1996) in *CRC Standard Mathematical Tables and Formulae* (Zwillinger, D., Ed.) pp 305−308, CRC Press, Boca Raton, FL.
24. Dougherty, D. A. (1996) *Science 271*, 163−168.
25. Scrutton, N. S., and Raine, A. R. C. (1996) *Biochem. J. 319*, 1−8.
26. Ma, J. C., and Dougherty, D. A. (1997) *Chem. Rev. 97*, 1303−1324.
27. Burley, S. K., and Petsko, G. A. (1986) *FEBS Lett. 203*, 139−143.
28. Singh, J., and Thornton, J. M. (1990) *J. Mol. Biol. 211*, 595−615.
29. Loewenthal, R., Sancho, J., and Fersht, A. R. (1992) *J. Mol. Biol. 224*, 759−770.
30. Dougherty, D. A. Personal communication.

BI980318S